ELSEVIER

Materials Science and Engineering B28 (1994) 55-60

MATERIALS SCIENCE & ENGINEERING B

Lattice strain relaxation of ZnS layers grown by vapour-phase epitaxy on (100) GaAs

N. Lovergine[a], G. Leo[a], A.M. Mancini[a], F. Romanato[b], A.V. Drigo[b], C. Giannini[c], L. Tapfer[c]

[a] *Dipartimento di Scienza dei Materiali, Università and Unitá GNSM-INFM di Lecce, Via per Arnesano, I-73100 Lecce, Italy*

[b] *Dipartimento di Fisica "G. Galilei", Università and Unità GNSM-INFM di Padova, Via Marzolo 8, I-35100 Padova, Italy*

[c] *Centro Nazionale di Ricerca e Sviluppo dei Materiali (CNRSM), S.S. 7 per Mesagne-km 7+300, I-72100 Brindisi, Italy*

Abstract

The structural characterization of ZnS epilayers grown on (100) GaAs by H_2 transport vapour-phase epitaxy is reported. High-resolution X-ray diffraction and ion channelling Rutherford backscattering spectrometric measurements were used to evaluate the overall crystalline perfection of the epilayers and the distortion and reciprocal orientation of the ZnS and GaAs lattices and to measure the epilayer built-in lattice strain. High crystalline quality can be achieved at the surface of relatively thick (above ca. 1 μm) ZnS layers, although a dense distribution of extended defects was observed close to the ZnS/GaAs interface. It turns out that the ZnS unit cell is orthorombically distorted, although its deviation from a purely tetragonal distortion is very small. Systematic measurements of the ZnS lattice strain were performed on the epilayers and the results were compared with the thermal strain value obtained by temperature-dependent X-ray diffraction measurements. The data indicate that the ZnS built-in lattice strain can be entirely ascribed to a thickness-dependent thermal strain contribution, the initial lattice misfit at the growth temperature being almost totally relaxed even for relatively thin epilayers. Finally, no appreciable strain was found for epilayer thicknesses above about 3 μm.

Keywords: ZnS epilayers; Strain relaxation; X-ray diffraction; Ion channeling

1. Introduction

The achievement of efficient UV and blue light-emitting diodes and lasers is one of the major challenges of today's optoelectronics technology. For this purpose, the use of wide-gap II-VI semiconducting compounds along with low-dimensional heterostructures is considered a viable technological route to the realization of such devices. Among other systems, ZnSe/ZnS [1], ZnCdS/ZnS [2] and ZnSTe/ZnS [3] based strained layer superlattices and multiple quantum wells have recently attracted much attention. However, the lack of high-quality, low-cost ZnS single-crystalline wafers requires the epitaxial growth of such heterostructures on high-quality ZnS buffer layers grown directly on GaAs substrates. Owing to a 4.3% lattice mismatch between ZnS and GaAs, misfit defects are expected to form at or close to the ZnS/GaAs interface of relatively thick epilayers. In addition, the amount of lattice and thermal mismatch-induced residual strains in the ZnS epilayers is strongly related to the type and distribution of these defects, and also to the basic mechanisms involved in the ZnS/GaAs strain relaxation.

In this paper, we report for the first time the results of a detailed structural characterization of the ZnS/GaAs heterostructure. High-resolution X-ray diffraction (XRD) and Rutherford backscattering spectrometery (RBS) in channelling conditions were used to evaluate the overall crystalline perfection of ZnS epilayers grown by vapour-phase epitaxy (VPE) on (100) GaAs substrates, and to determine the precise deformation and reciprocal orientation of the ZnS and GaAs lattices. The crystalline quality of the epilayers was investigated as a function of their thickness, allowing a certain appreciation of the epilayer defect

SSDI 0921-5107(94)00801-9

distribution close to the ZnS/GaAs interface. Also, the amount of built-in lattice strain occurring into each ZnS layer was precisely measured and compared with the expected thermal strain value, as measured by temperature-dependent XRD. This allowed us to discriminate between lattice and thermal mismatch-induced strains, whose relative contributions to the measured built-in lattice strain were thus determined.

2. Experimental details

The ZnS epilayers were grown by the H_2 transport VPE method [4] in a horizontal chamber, two temperature zone reactor, designed and built by our group for the epitaxy of II–VI compounds, as described elsewhere [5]. A nominally stoichiometric 5N purity ZnS source from Cerac was used as the starting material. Semi-insulating (resistivity $> 10^7$ Ω cm) (100) $\pm 0.50°$ oriented GaAs substrates supplied by Sumitomo were used throughout. Immediately before loading into the reactor, the substrates were first degreased in isopropanol vapour and then etched in H_2SO_4–H_2O_2–H_2O (4:1:2) solution for 10 min at around 40 °C, thoroughly rinsed in deionized water and finally dried under a flow of pure nitrogen. In order to remove any residual oxide from the GaAs surface, an in situ thermal treatment was routinely applied to the substrates at around 600 °C for 5 min under a 300 standard cm^3 min^{-1} (sccm) total flow of hydrogen. The ZnS epilayers were grown at 650 °C under a 300 sccm flow of hydrogen through the chamber, the source temperature being kept fixed at 750 °C. These conditions gave a ZnS average growth rate of about 1.0 μm h^{-1}. Several ZnS epilayers were deposited, their thicknesses ranging between 130 nm and 4.1 μm. Immediately after the end of the growth, the samples were quickly (< 5 min) cooled to room temperature under a 200 sccm flow of pure nitrogen.

XRD experiments were performed on the ZnS/GaAs samples to determine the heterostructure lattice strain distortions and orientation by using a high-resolution diffractometer in a double axis (DA) Bragg configuration, equipped with a Cu Kα line-emitting X-ray tube, a four-reflection (220) Ge monochromator having a final beam angular divergence of 12" and a proportional counter. Also, temperature-dependent lattice strain measurements in a single-axis (SA) mode were performed on a few samples by means of a single-crystal diffractometer, equipped with a high-temperature, low-vacuum (10^{-3} Torr) chamber, a Cu Kα line-emitting X-ray tube and a proportional counter. For this purpose, the ZnS/GaAs samples were mounted on a current-heated tantalum strip and their temperature was precisely controlled (within ± 2 °C) by a thermocouple.

Rutherford backscattering spectrometry in both random and ion channelling geometry was performed systematically on all ZnS/GaAs samples. A $^4He^+$ beam, whose energy ranged between 2.0 and 3.5 MeV, was used to record the RBS spectra. Angular yield curves for a surface region were recorded for several lattice directions inclined to the surface normal. For this purpose, a goniometer having both a repeatability and an overall precision of 0.01° was used for the channelling measurements [6].

Finally, a quantitative evaluation of the ZnS surface roughness was obtained from the present samples by using a Tencor Instruments Model 200 Alpha-step surface profiler having a vertical resolution of 0.5 nm and a corresponding lateral resolution of about 40 nm. Several 40 μm surface scans were performed at a 25 point μm^{-1} sampling rate for each ZnS sample and the surface heights along the scan lines were recorded. This allowed the calculation of the ZnS surface average roughness R_a, i.e. the arithmetic average of the surface hight deviations from the mean surface height along the scan line [7].

3. Results and discussion

Ion channelling RBS measurements were performed on different samples to estimate the ZnS epilayer surface crystalline quality. Fig. 1 shows typical RBS spectra recorded for a 570 nm thick ZnS layer in both [100]-aligned and random geometry. The energy to depth conversion for the experimental conditions used

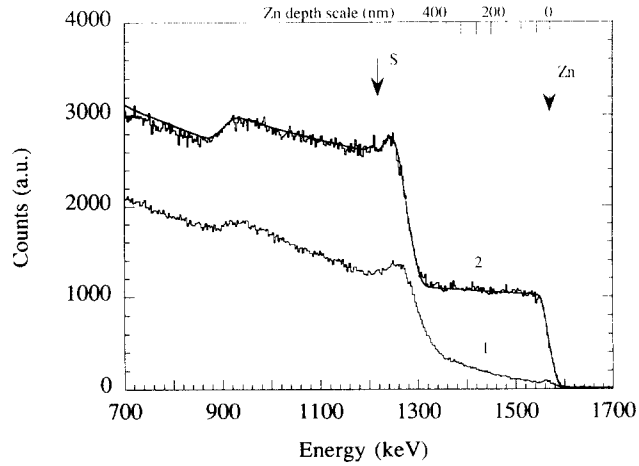

Fig. 1. Typical 2.0 MeV $^4He^+$ RBS spectra of a 570 nm thick ZnS epilayer: (1) [100]-aligned; (2) random geometry. The solid line superposed on the random spectra is the corresponding RBS simulation.

was obtained by using the stopping power of Ref. [8]. A certain estimation of the crystalline perfection is given by the surface minimum yield of the aligned spectrum χ_{min}, i.e. the aligned yield just behind the Zn surface peak normalized to the random yield. Fig. 2 shows the values of χ_{min} as a function of the epilayer thickness. For ZnS thicknesses above about 1 μm our measurements indicate an almost constant value of χ_{min} around 5%, which is close to the theoretical predictions for a perfect ZnS crystal [9]. However, below 1 μm the χ_{min} value increases monotonically with decreasing epilayer thickness, indicating the occurrence of a high-defect region close to the ZnS/GaAs interface.

Simulations of the RBS spectra in random geometry show that a fairly good agreement with the corresponding experimental spectra can only be achieved by introducing an interfacial linearly graded composition profile between ZnS and GaAs over a specific thickness Δt (composition tail), whose value is reported in

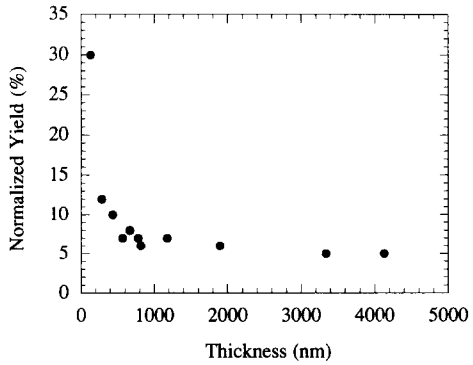

Fig. 2. Values of the [100]-aligned RBS minimum yield χ_{min} as a function of the ZnS epilayer thickness.

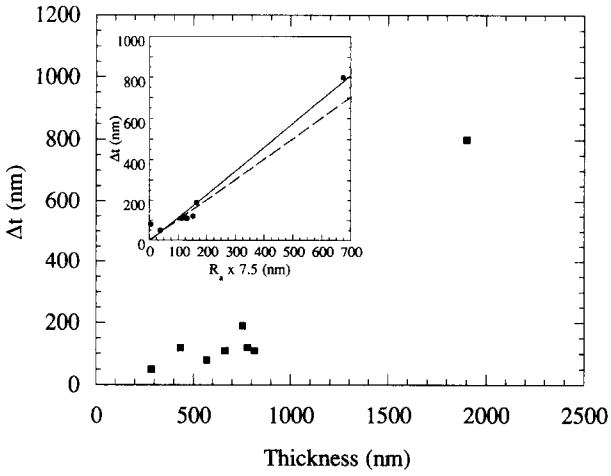

Fig. 3. Composition tail values Δt, as determined from simulation of the RBS random spectra, as a function of the ZnS epilayer thickness. The correlation between Δt and the gaussian full width of the epilayer thickness distribution $6\sigma = 7.5R_a$ is shown in the inset, where the solid line is the linear best fit of the experimental data and the dashed line represents the $\Delta t = 6\sigma$ relationship.

Fig. 3 as a function of the ZnS epilayer thickness. In this respect, although the RBS technique does not discriminate between elemental interdiffusion and interface or surface roughness-induced effects, it appears that our Δt values show a superlinear dependence on the epilayer thickness, the latter being in turn proportional to the growth time. This clearly indicates that interdiffusion is not the main source of the observed RBS composition tail. In addition, surface profiling measurements showed that the ZnS surface average roughness R_a follows a dependence on the epilayer thickness similar to that shown by Δt. Assuming a Gaussian distribution for the epilayer thickness with a standard deviation $\sigma = 1.25R_a$ around the mean thickness value, a correlation is found between Δt and the full width of the thickness distribution. This is shown in the inset in Fig. 3, where the values of Δt are reported as a function of the gaussian full width 6σ. It appears that our Δt values vary linearly with the sample R_a, although they are slightly higher than expected on the basis of the ZnS surface roughness. In this respect, it must be noted that the finite size of the surface profiler stylus results in values of σ which are underestimated with respect to the real values, possibly explaining the observed deviations, although the value of 6σ assumed for the gaussian full width is somewhat arbitrary and could be reduced to 4σ on taking into account the difficulty in evaluating the tail of the thickness distribution. Although the ZnS surface roughness appears to be the dominant source of the observed RBS composition tail, we cannot rule out the presence of a small contribution arising from elemental interdiffusion at the ZnS/GaAs interface. Indeed, the occurrence of such interdiffusion has been confirmed by secondary ion mass spectrometric measurements [10].

Fig. 4 shows two DA θ–2θ scans recorded at two different positions across a ZnS/GaAs sample in the angular range between the (400) reflections of GaAs and ZnS. It appears that the ZnS (400) reflections peaks are much broader then expected for an ideal ZnS epilayer of the same thickness, this fact being clearly related to the occurrence of defects in the epilayer, in agreement with the above ion channelling results. Also, the measured full width at half maximum (FWHM) values of the ZnS peaks decrease monotonically with the epilayer thickness, as shown in the inset in Fig. 4. To our knowledge, the crystalline perfection of the present epilayers is comparable to the best ZnS epilayer quality reported in the literature.

A significant difference can be observed between the two spectra in Fig. 4 on the low-angle side of the GaAs Bragg peaks. While the same GaAs peak position is found, a distinctive broadening appears in one of the two spectra, this effect being observed also for the

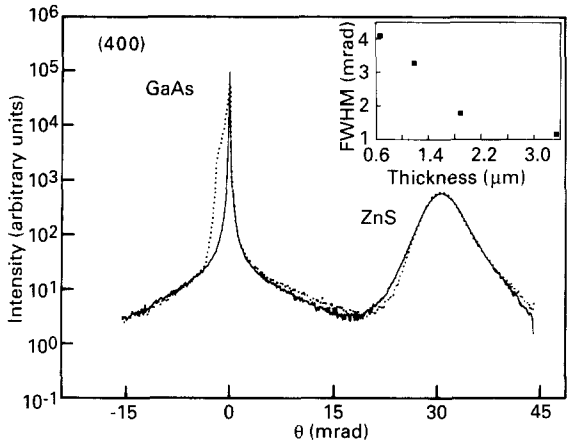

Fig. 4. Two double-axis XRD spectra (θ–2θ scans) recorded in the vicinity of the (400) reflections of a ZnS/GaAs sample. The two spectra correspond to diffraction mesurements performed by impinging the X-ray beam on different regions of the sample. The inset shows the FWHM values of the ZnS (400) peak as a function of the epilayer thickness.

Table 1
Values of the strain tensor components (ε_{ij}) and lattice rotation parameters (U_{ij}) obtained by DA high-resolution XRD measurements performed on two ZnS/GaAs samples

Parameter	Sample 39[a]	Sample 27[a]
ε_{zz}	$-(4.417\pm0.004)\times10^{-2}$	$-(4.415\pm0.003)\times10^{-2}$
ε_{xx}	$-(4.283\pm0.006)\times10^{-2}$	$-(4.222\times0.006)\times10^{-2}$
ε_{yy}	$-(4.217\pm0.006)\times10^{-2}$	$-(4.244\pm0.006)\times10^{-2}$
ε_{xz}	$(1.0\pm0.5)\times10^{-4}$	$-(1.2\pm0.5)\times10^{-5}$
ε_{yz}	$(0\pm5)\times10^{-5}$	$-(2.9\pm0.5)\times10^{-5}$
U_{zx}	$(0\pm2)\times10^{-5}$	$(0\pm2)\times10^{-5}$
U_{zy}	$(0\pm2)\times10^{-5}$	$(0\pm2)\times10^{-5}$

[a]The ZnS thicknesses are 655 and 1180 nm for samples 39 and 27 respectively, as determined by RBS simulation.

asymmetric (422) reflections. In this respect, preliminary isointensity contour mapping around the GaAs (400) reciprocal lattice point shows that defects occur at the surface of the GaAs wafers. In fact, a diffused X-ray scattering around the (400) lattice point has been observed on both as-received and etched GaAs substrates. In the latter case, such scattering is weaker and rather inhomogeneous across the sample with respect to the untreated substrates, indicating that, although the etch treatment removes several micrometres of GaAs, a residual amount of defects remains at the surface of the GaAs substrates. We suggest that the GaAs peak broadening in Fig. 4 is related to such an inhomogeneous density of residual defects, although the observed interface diffusion between ZnS and GaAs could further contribute to this effect.

A detailed analysis of the ZnS lattice distortion was carried out on several ZnS/GaAs samples by means of DA high-resolution XRD measurements. For this purpose, rocking curves were recorded in the vicinity of the (400), (422), (4$\bar{2}$2), (4$\bar{2}\bar{2}$), (42$\bar{2}$), (531) and (5$\bar{3}\bar{1}$) reflections and for several azimuthal angles, the ZnS peak angular positions being determined (within $\pm3\times10^{-2}$ mrad) by gaussian lineshape fitting of the diffraction spectra. To analyse the diffraction data we used second-order approximation of the strain function in the Takagi–Taupin equation, assuming the most general distortion (i.e. triclinic) for the ZnS unit cell [11,12]. In this model the lattice distortion is described in terms of a (3×3) strain and a (3×3) rotation tensor, taking into account both the cell distortion and rotation with respect to the substrate unit cell. Table 1 reports the results of our analysis for two ZnS/GaAs samples [10], where ε_{xx}, ε_{yy} and ε_{zz} are the tensile strain components, ε_{xz} and ε_{yz} are the shear strain components and U_{zx} and U_{zy} are the cell rotation parameters. The reported tensor component errors were precisely calculated by applying the Gaussian error propagation law to the epilayer-to-substrate peak angular distance uncertainties, as determined from rocking curves lineshape fitting. It appears that the ZnS lattice is always parallel to the GaAs substrate. Also, an appreciable built-in tensile strain was found for all of the samples examined, the shear strain components being zero or vanishingly small in most cases. Our data indicate that the in-plane tensile strain components ε_{xx} and ε_{yy} are systematically slightly different from each other, implying an orthorhombic deformation of the ZnS unit cell. This result can be explained by the occurrence of a small asymmetry in the distribution of the misfit dislocation Burger vectors along the [011] and [0$\bar{1}$1] directions at the ZnS/GaAs interface, according to Ref. [13]. Finally, for one sample, DA XRD measurements were performed at different points where the GaAs peak broadening occurred and compared with rocking curves obtained from points where that effect was not observed. It turned out that the tensile strain components remain the same (within experimental error) for all cases.

Although the high-resolution XRD measurements above indicate that the ZnS unit cell distortion is orthorhombic, the differences between the in-plane ε_{xx} and ε_{yy} strain components are negligible with respect to the strain measurement precision of the ion channelling technique. Therefore, a tetragonal distortion approximation for the ZnS unit cell was assumed for the present ion channelling strain measurements. Values of the tetragonal distortion $\varepsilon_T = a_\perp/a_\parallel - 1$, where $a_\perp$ and $a_\parallel$ are the ZnS lattice parameters normal and parallel to the ZnS/GaAs interface, respectively, were obtained by measuring the angular deviations of lattice direc-

tions inclined on the surface normal with respect to the corresponding directions in the unstrained lattice [6].

Our data show that the ion channelling ε_T values coincide, within the experimental uncertainties, with the corresponding high-resolution XRD values, obtained by assuming the relationship $\varepsilon_T = (\varepsilon_{zz} - \varepsilon_{xx,yy})/(\varepsilon_{zz} + 1)$ between the epilayer tetragonal strain and the heterostructure strain tensor components [14]. We can thus define the ZnS in-plane (parallel) strain $\varepsilon_\parallel = -\varepsilon_T/(1+\alpha)$, the value of $\alpha = 2C_{12}/C_{11}$ being about 1.28 for ZnS [15].

Systematic ion channelling measurements of the epilayer surface strain $\varepsilon_\parallel$ were performed on several ZnS/GaAs samples and compared with the thermal strain value $\varepsilon_{\Delta T} = (1.3 \pm 0.3) \times 10^{-3}$, independently measured by SA XRD performed on a relatively thin sample between room temperature and 650 °C [10]. The results are shown in Fig. 5, where the values of $\varepsilon_\parallel$ are reported as a function of the ZnS epilayer thickness. The value of $\varepsilon_{\Delta T}$ is also given. It appears that the tensile parallel strain decreases monotonically with increasing ZnS thickness, always remaining below the thermal strain value except for the thinnest (310 nm) of the samples examined, whose $\varepsilon_\parallel$ value coincides, within experimental error, with $\varepsilon_{\Delta T}$. This indicates that the tensile strain value observed in the 310 nm thick epilayer can be entirely ascribed to the thermal strain contribution, the residual ZnS lattice strain occurring in this sample thus being smaller than 1×10^{-4} if not zero. Therefore, we conclude that the initial ZnS/GaAs heterostructure lattice misfit (ca. 4.2% at the growth temperature) has most relaxed in our ZnS epilayers.

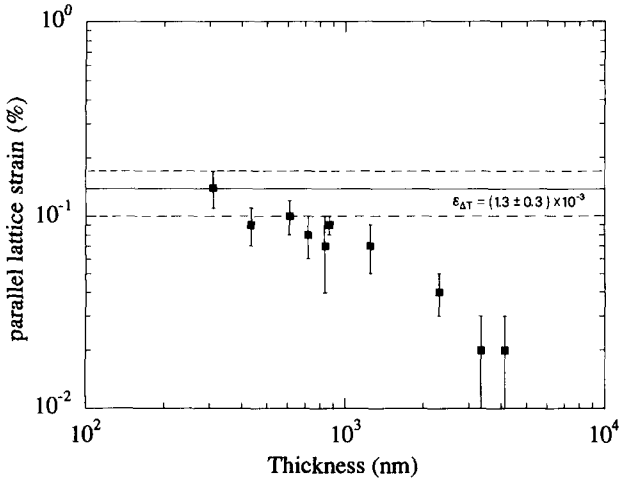

Fig. 5. Tensile parallel lattice strain obtained by ion channelling measurements as a function of the ZnS epilayer thickness. The horizontal solid line represents the thermal strain value $\varepsilon_{\Delta T}$, as determined by temperature-dependent XRD, its lower and upper limits being indicated by the two dashed lines.

Moreover, the decrease of the overall tensile strain with the epilayer thickness shown by our ion channelling data indicates that around 430 nm even the thermal strain begins to relax, until no appreciable strain remains for ZnS thicknesses above about 3 μm.

4. Conclusions

We have reported the structural characterization of ZnS epilayers grown on (100) GaAs by H_2 transport VPE. High-resolution XRD and ion channelling RBS measurements were used to evaluate the overall crystalline perfection of the epilayers. High crystalline quality can be achieved at the surface of relatively thick (above ca. 1 μm) ZnS layers, although a dense distribution of extended defects was observed in a thin epilayer region close to the ZnS/GaAs interface. A detailed analysis of the high-resolution XRD measurements performed on the present samples allowed the determination of the distortion and orientation of the ZnS unit cell. It turned out that the ZnS and GaAs lattices are parallel to each other, the ZnS unit cell being orthorhombically distorted, although its deviation from a purely tetragonal distortion is very small. Systematic ion channelling measurements of the built-in ZnS lattice strain were therefore performed on epilayers having different thicknesses and compared with the thermal strain value obtained by temperature-dependent XRD measurement. Our data indicate that the measured ZnS built-in lattice strain can be entirely ascribed to a thickness-dependent thermal strain contribution, the initial lattice misfit at the growth temperature being almost totally relaxed even for relatively thin layers.

References

[1] T. Taguchi, Y. Kawakami and Y. Yamada, *Physica B, 191* (1993) 23.
[2] Y. Yamada, Y. Masumoto and T. Taguchi, *Physica B, 192* (1993) 83.
[3] T. Yokogawa, *Physica B, 191* (1993) 102.
[4] S. Iida, T. Sugimoto, S. Suzuki, S. Kishimoto and Y. Yagi, *J. Cryst. Growth, 72* (1985) 51.
[5] A.M. Mancini, N. Lovergine, C. De Blasi and L. Vasanelli, *Nuovo Cimento D, 10* (1988) 57.
[6] A.Carnera and A.V. Drigo, *Nucl. Instrum. Methods, B44* (1990) 357.
[7] *ANSI Specifications No. B46*, I-1978.
[8] J. Ziegler, *Stopping and Ranges of Ions in Matter*, Vol. 4, Pergamon, New York, 1977.
[9] D.S. Gemmel and R.C. Mikkelson, *Phys. Rev. B, 6* (1972) 1613.
[10] C. Giannini, T. Peluso, D. Gerardi, L. Tapfer, N. Lovergine

and L. Vasanelli, *J. Appl. Phys.*, submitted for publication.
[11] C.Giannini, L. De Caro and L.Tapfer, *Solid Sate Commun.*, submitted for publication.
[12] Yu. P. Khapachev and F.N. Chukhovskii, *Sov. Phys. Crystall., 34* (1989) 465.
[13] M. Mazzer, A. Carnera, A.V. Drigo and C. Ferrari, *J. Appl. Phys., 68* (1990) 531.
[14] A. Armigliato, M. Servidori, F. Cembali, R. Fabbri, R. Rosa, F. Corticelli, D. Govoni, A.V. Drigo, M. Mazzer, F. Romanato, S. Frabboni, R. Balboni, S.S. Iyer and A. Guerrieri, *Microsc. Microanal. Microstruct., 3* (1992) 363.
[15] H. Hartmann, R. Mach and B. Selle, in E. Kaldis (ed.), *Current Topics in Materials Science*, Vol. 9, North-Holland, Amsterdam, 1982, p. 36.